Optimization under uncertainty of a hybrid waste tire and natural gas feedstock flexible polygeneration system using a decomposition algorithm

Authors:

Avinash Subramanian, Rohit Kannan, Flemming Holtorf, Thomas A. Adams II, Truls Gundersen, Paul I. Barton

Date Submitted: 2021-11-01

Keywords: Polygeneration system, Waste-to-Energy, Stochastic Programming, Decomposition Algorithm, Waste Tire, Optimization under uncertainty

Abstract:

Market uncertainties motivate the development of flexible polygeneration systems that are able to adjust operating conditions to favor production of the most profitable product portfolio. However, this operational flexibility comes at the cost of higher capital expenditure. A scenario-based two-stage stochastic nonconvex Mixed-Integer Nonlinear Programming (MINLP) approach lends itself naturally to optimizing these trade-offs. This work studies the optimal design and operation under uncertainty of a hybrid feedstock flexible polygeneration system producing electricity, methanol, dimethyl ether, olefins or liquefied (synthetic) natural gas. The recently developed GOSSIP software framework is used for modeling the optimization problem as well as its efficient solution using the Nonconvex Generalized Benders Decomposition (NGBD) algorithm. Two different cases are studied: The first uses estimates of the means and variances of the uncertain parameters from historical data, whereas the second assesses the impact of increased uncertain parameter volatility. The value of implementing flexible designs characterized by the value of the stochastic solution (VSS) is in the range of 260 - 405 M$ for a scale of approximately 893 MW of thermal input. Increased price volatility around the same mean results in higher expected net present value and VSS as operational flexibility allows for asymmetric exploitation of price peaks.

Record Type: Preprint

Submitted To: LAPSE (Living Archive for Process Systems Engineering)

Citation (overall record, always the latest version):	LAPSE:2021.0798
Citation (this specific file, latest version):	LAPSE:2021.0798-1
Citation (this specific file, this version):	LAPSE:2021.0798-1v1

Optimization under uncertainty of a hybrid waste tire and natural gas feedstock flexible polygeneration system using a decomposition algorithm

Avinash S.R. Subramanian[a], Rohit Kannan[b], Flemming Holtorf[c], Thomas A. Adams II[d], Truls Gundersen[a], Paul I. Barton[c]

[a]*Department of Energy and Process Engineering, Norwegian University of Science and Technology (NTNU), Kolbjørn Hejes vei 1B, NO-7491, Trondheim, Norway.*
[b]*Center for Nonlinear Studies and Theoretical Division (T-5), Los Alamos National Laboratory, Los Alamos, NM 87545 USA.*
[c]*Process Systems Engineering Laboratory, Department of Chemical Engineering, Massachusetts Institute of Technology, 77 Massachusetts Avenue, Cambridge, Massachusetts 02139, United States.*
[d]*Department of Chemical Engineering, McMaster University, 1280 Main St. W, Hamilton, ON, Canada, L8S 4L7.*

Abstract

Market uncertainties motivate the development of flexible polygeneration systems that are able to adjust operating conditions to favor production of the most profitable product portfolio. However, this operational flexibility comes at the cost of higher capital expenditure. A scenario-based two-stage stochastic nonconvex Mixed-Integer Nonlinear Programming (MINLP) approach lends itself naturally to optimizing these trade-offs. This work studies the optimal design and operation under uncertainty of a hybrid feedstock flexible polygeneration system producing electricity, methanol, dimethyl ether, olefins or liquefied (synthetic) natural gas. The recently developed GOSSIP software framework is used for modeling the optimization problem as well as its efficient solution using the Nonconvex Generalized Benders Decomposition (NGBD) algorithm. Two different cases are studied: The first uses estimates of the means and variances of the uncertain parameters from historical data, whereas the second assesses the impact of increased uncertain parameter volatility. The value of implementing flexible designs characterized by the value of the stochastic solution (VSS) is in the range of 260 - 405 M$ for a scale of approximately 893 MW of thermal input. Increased price volatility around the same mean results in higher expected net present value

Preprint submitted to Energy/Applied Energy/I&ECR/Comp. Chem. TBDNovember 1, 2021

and VSS as operational flexibility allows for asymmetric exploitation of price peaks.

Keywords: Polygeneration system, Waste-to-Energy, Stochastic Programming, Decomposition Algorithm, Waste Tire, Optimization under uncertainty

1. Introduction

Polygeneration involves the production of multiple products such as a mix of electricity, fuels (gasoline, diesel, synthetic natural gas, hydrogen) and chemicals (methanol, dimethyl ether, olefins, acetic acid) in the same location. One pertinent strategy is to also use multiple complementary feedstocks in order to exploit certain synergies, for instance, by generating syngas of different qualities that can be blended to provide the correct H_2/CO ratio for downstream synthesis, sharing of upstream equipment or heat integration of exothermic and endothermic processing units [1, 2]. In addition, including an alternative feedstock such as waste tire [3, 4], plastics, municipal solid waste [5] or petcoke [6, 7] may allow energy companies to lower their overall environmental impact while also mitigating energy security concerns. The use of wastes is particularly important because increased population growth is expected to create larger waste quantities that require appropriate management. For instance, in the developed world, approximately 1 waste tire per person per year is produced resulting in approximately 1 billion discarded tires annually [8]. In addition, there are currently an estimated 4 billion waste tires in landfills and stockpiles worldwide. In this paper, we study the use of waste tires because they are a particularly suitable feedstock for conversion to high-value products through gasification as a result of their homogeneous nature, high energy density (Lower Heating Value of ~ 33.96 MJ/kg, higher than coal), high volatile matter content ($\sim 67\%$) and low ash content ($\sim 7\%$) [9].

A further development to the polygeneration concept is to implement a flexible design which involves oversizing process equipment so as to allow adjustment of the production rates (and thus the product portfolio) in order to exploit market volatility. Thus, the flexible design problem involves optimizing the trade-offs between the increased capital costs associated with the larger equipment capacities and the expected increase in profit due to operational flexibility. This optimization problem can be formulated as a scenario-

based two-stage stochastic Mixed-Integer Nonlinear Program (MINLP) as explained in Section 2.1. The choice of equipment sizes is modeled using discrete first-stage variables (fixed before the realization of uncertainty) and the operating conditions are modeled using continuous second-stage variables (adjusted in response to realization of uncertainty). This optimization problem is typically nonconvex as a result of the nonlinear equations necessary to describe mixing, splitting and chemical reaction processes.

Such two-stage stochastic programs with recourse exhibit a special structure that makes them amenable to solution using duality-based decomposition approaches. For instance, the Benders decomposition (or L-shaped method) provides an efficient approach for solution of two-stage stochastic Mixed-Integer Linear Programs (MILPs) [10]. This strategy was extended to give the Generalized Benders Decomposition (GBD) algorithm that can solve two-stage stochastic Mixed-Integer Convex Programs (MICPs) [11]. However, nonconvex optimization problems generally do not satisfy strong duality, thus convergence cannot be guaranteed with GBD. This motivated Li et al. [12, 13] to develop the Nonconvex Generalized Benders Decomposition (NGBD) algorithm used in this paper which is summarized in Section 2.2. The NGBD algorithm is guaranteed to solve two-stage stochastic nonconvex MINLPs with discrete first-stage variables to global optimality. Furthermore, we use the GOSSIP software (recently developed by Kannan and Barton) that provides a versatile framework for modeling two-stage stochastic nonconvex MINLPs as well as their efficient solution using the NGBD algorithm [14].

Previous work on flexible polygeneration was done by Meerman et al. who studied the conversion of coal, biomass and oil residues to hydrogen, Fischer-Tropsch liquids, methanol, urea and electricity [15, 16]. The economic value of implementing various levels of flexibility was determined and an analysis on the favored feedstocks and products for each price scenario was presented. However, an optimization of the system design and operating conditions was not carried out. Farhat and Reichelstein presented a first-principles analysis on the economic performance of flexible polygeneration using a simplified case study of a coal to electricity and fertilizers process [17]. They derived a series of propositions to quantify the "value of flexible polygeneration" which could be subdivided into the "value of diversification" and "value of flexibility". While these propositions provide useful intuition, they only hold for flow sheets without interconnections (where the flow sheet could be represented as a tree) and no detailed process design or optimization was done. Chen et al. studied the optimal design and operation of a pro-

cess in which coal and biomass are co-gasified to produce a mix of naphtha, diesel, methanol or electricity [18]. The optimization problem was formulated first as a two-stage stochastic nonconvex Nonlinear Program (NLP) with a concave objective function and solved with BARON. In order to satisfy the requirement of having only discrete first-stage variables, the optimization problem was reformulated as an MINLP and solved using the NGBD algorithm enhanced with additional dual information [19]. Both feedstocks were converted in a single gasification unit, thus the option of generating multiple syngas streams followed by subsequent blending was not studied.

While the studies presented above highlight the value of implementing a flexible design for polygeneration processes, further research is necessary on the co-utilization of waste tires and natural gas. These feedstocks are converted into separate syngas streams of different qualities that can then be blended in appropriate ratios so as to exploit available synergies. Furthermore, this work studies the influence of the degree of market volatility on the expected profitability of the flexible polygeneration process. Thus, the objective of this paper is to study the optimal design and operation under uncertainty of such a hybrid feedstock flexible polygeneration system with a product portfolio consisting of electricity, methanol, dimethyl ether, olefins or liquefied (synthetic) natural gas.

This paper is organized as follows: Section 2 provides a brief overview of the two-stage stochastic programming approach for optimization under uncertainty, the GOSSIP software framework and the NGBD algorithm; Section 3 details the approach for process modeling and formulation of the optimization under uncertainty problem; Section 4 presents the results and a discussion of the computational performance of the NGBD algorithm versus the state-of-the-art ANTIGONE solver. We present our conclusions in Section 5.

2. Optimization under uncertainty

2.1. General structure of two-stage stochastic nonconvex MINLPs

Designing a flexible polygeneration process involves determining the optimal trade-offs between the increased capital costs as a result of over-sizing the process equipment and the increased net profit as a result of operational flexibility to exploit price peaks. In this work, we use the two-stage stochastic programming approach [20] to place these two trade-offs on a level basis. Two-stage stochastic programming divides the decision variables into two

categories: First-stage or design decision variables that are made before the realization of uncertainty and cannot be altered after plant construction and second-stage or operational variables that can be adjusted after the realization of uncertainty during the plant life time. Thus, first-stage variables correspond to the choice of equipment sizes while second-stage variables correspond to operating conditions (such as flow rates, split fractions etc.) for each scenario of uncertain parameters. A recent review of stochastic programming approaches for optimization of process systems under uncertainty is presented by Li and Grossmann [21].

In particular, the flexible design problem is formulated as a two-stage stochastic MINLP with a structure presented in Problem (SP), where $\mathbf{y}$ denotes the first-stage design decision variables; $\mathbf{x}_h$, p_h, $\boldsymbol{\omega}_h$ denote the second-stage operational decision variables, probability of occurrence and realization of the uncertain parameter vector in scenario h respectively; $\mathbf{c}$ denotes a vector corresponding to capital cost data and f_h is the objective function of the second-stage (recourse) problem indexed by scenario h (corresponding to the operating profit in that scenario); data matrix $\mathbf{A}$ and vector $\mathbf{b}$ define constraints on the first-stage variables; data matrix $\mathbf{B}$ and the functions $\mathbf{g}_h$ are used to represent scenario-dependent constraints; $\boldsymbol{Y}$ and $\boldsymbol{X}_h$ correspond to the bounds on $\mathbf{y}$ and $\mathbf{x}_h$ respectively. We note that the uncertain parameters are modeled using a random vector with finite support i.e., the vector of uncertainty parameters can take on one of a finite number of scenarios s, where $h \in \{1,...,s\}$ indexes the scenario set. Thus Problem (SP) corresponds to the deterministic equivalent problem.

$$
\begin{aligned}
\max_{\mathbf{y},\mathbf{x}_1,\ldots,\mathbf{x}_s} \quad & \mathbf{c}^{\mathrm{T}}\mathbf{y} + \sum_{h=1}^{s} p_h f_h(\mathbf{x}_h, \boldsymbol{\omega}_h) \\
\text{s.t.} \quad & \mathbf{A}\mathbf{y} \leq \mathbf{b}, \\
& \mathbf{B}\mathbf{y} + \mathbf{g}_h(\mathbf{x}_h, \boldsymbol{\omega}_h) \leq \mathbf{0}, \qquad \forall h \in \{1,...,s\}, \\
& \mathbf{y} \in \boldsymbol{Y}, \\
& \mathbf{x}_h \in \boldsymbol{X}_h, \qquad \forall h \in \{1,...,s\}
\end{aligned}
\tag{SP}
$$

We note that the flexible design problem (SP) satisfies the following assumptions (although the NGBD algorithm is more generally applicable [13]):

1. All first-stage variables are bounded and discrete and thus can be reformulated using binary variables and additional linear constraints i.e.,

$\mathbf{y} \in \{0,1\}^{n_y}$, where n_y denotes the number of first-stage variables. This requirement needs to be satisfied for guaranteed convergence of the NGBD algorithm.

2. All second-stage variables $\mathbf{x}_h$ are continuous.
3. All participating functions are assumed to be factorable (i.e., they can be expressed as a finite recursive composition of certain univariate and bivariate functions as detailed in [22])
4. All participating functions are assumed to be separable in the (first-stage) binary and (second-stage) continuous variables. In addition, the capital cost data are not subject to uncertainty and all participating functions are assumed to be affine in $\mathbf{y}$.

The objectives, process model and constraints of the flexible design problem are translated into the form of Problem (SP) as described in Section 3.

2.2. Overview of the NGBD algorithm and the GOSSIP software framework

Two-stage stochastic programs exhibit a special structure: The first-stage variables of Problem (SP) are complicating variables in the sense that fixing them allows the original optimization problem to be separated into a number of smaller independent subproblems. This suggests a solution approach that involves iterating between searching the space of first-stage variables followed by the space of second-stage variables. Geoffrion outlines a two-step conceptual framework for the synthesis of efficient mathematical programming algorithms based on this intuition: First, the original problem is manipulated (using techniques such as projection, dualization, inner linearization and outer linearization) to derive an equivalent "Master Problem" that is easier to solve, and second, solution strategies (such as piecewise, relaxation and restriction) are employed to reduce the master problem to a sequence of subproblems that ideally can be solved using efficient specialized solvers [23]. Duality-based decomposition approaches are an illustration of this strategy: For instance, the GBD algorithm can be viewed as a procedure of applying projection and dualization followed by relaxation and restriction [11, 24].

The NGBD algorithm is a generalization of the GBD algorithm to the class of problems containing participating functions that are nonconvex in the second-stage variables. The general principle is to iteratively solve a series of lower bounding and upper bounding problems until convergence to a globally optimal solution (within a specified tolerance). The lower bounding problem is formulated by convexifying the original problem (SP). The

current implementation employs the Auxiliary Variable Method detailed in [25] although alternative approaches based on McCormick relaxations [22] (or the differentiable variant [26]) could also be implemented. The GBD algorithm is used to solve the lower bounding problem. Once GBD converges with a solution to the lower bounding problem, an upper bounding problem is constructed by fixing the $\mathbf{y}$ variables to this lower bounding solution. This yields a nonconvex NLP that is also fully decomposable by scenario. Affine inequalities are added to the lower bounding problem to exclude previously visited solutions $\mathbf{y}$ and the procedure is iterated until convergence [27].

In order to provide a versatile framework for the formulation of two-stage stochastic nonconvex MINLPs and their efficient solution using the NGBD algorithm, the GOSSIP software was recently developed as detailed in [14]. A native C++-based modeling language is provided for the user to formulate an optimization problem which can be of the form of Problem (SP). Subroutines for parsing the user-defined model as well as pre-processing are implemented. In addition, subroutines for automatic construction of all the necessary subproblems for the NGBD algorithm as well as links to state-of-the-art optimization solvers for their solution are implemented. A link to ANTIGONE is also implemented to solve the deterministic equivalent problem without using a decomposition strategy [28].

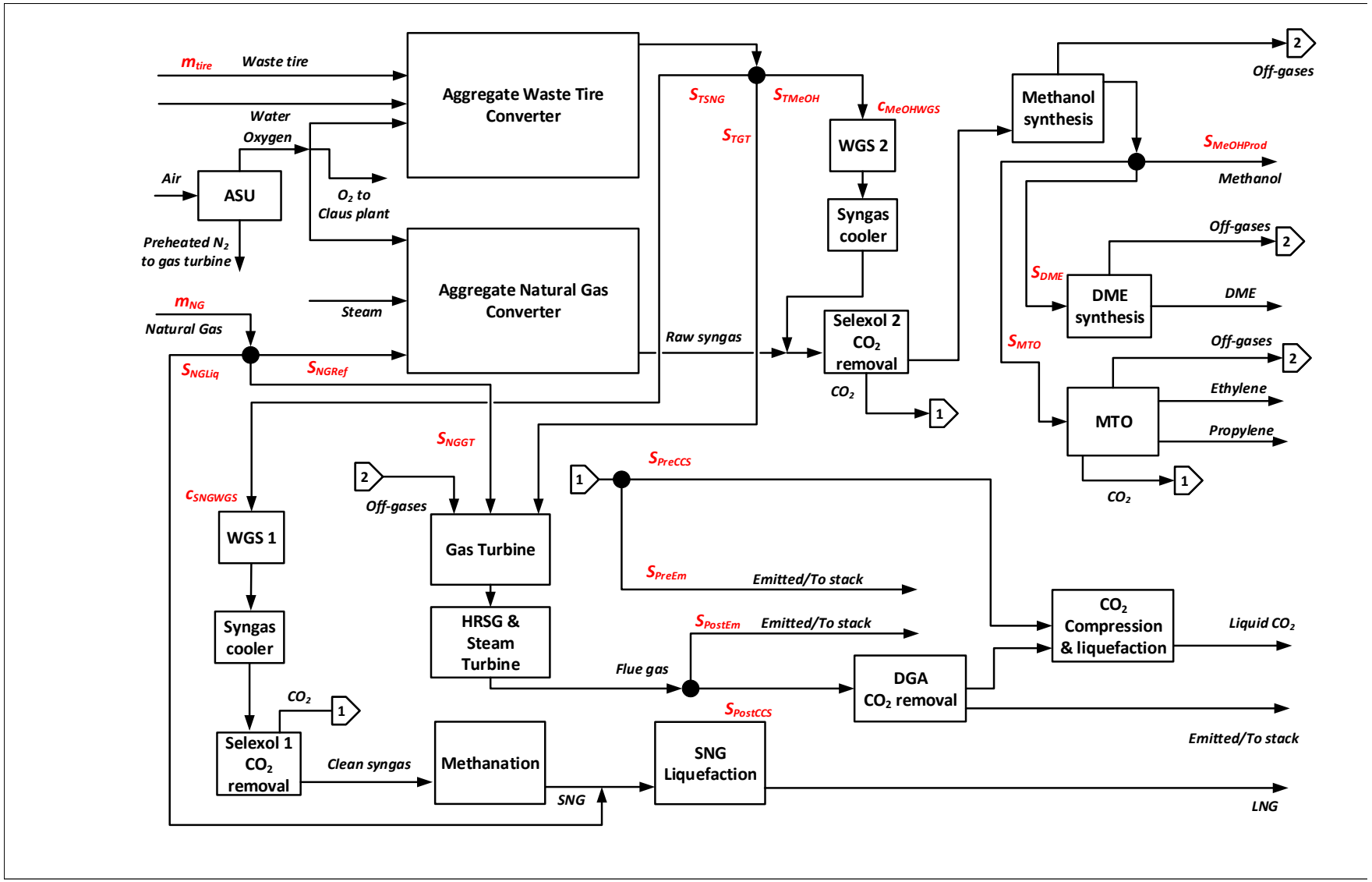

Figure 1: Superstructure of the hybrid natural gas and waste tire feedstock polygeneration system. The operational decision variables are indicated in red and presented in Table 2

Unit	Parameters	Reference
Tire Feedstock	Ultimate (wt%): C: 77.3, H: 6.2, N: 0.6, S: 1.8, O: 7.3, Ash: 6.8	[3]
	Proximate (wt%): VM: 67.7, FC: 25.5, Ash: 6.8	
Natural Gas (NG) Feedstock	T = 30 °C, P = 30 bar	[29]
	Composition (mol%): CH_4: 93.9, N_2: 0.008, CO_2: 0.01, C_2H_6: 0.032, C_3H_8: 0.007, C_4^+: 0.004	
Waste Tire Converter		
Waste tire preparation	Crumb size = 0.18 mm	[30]
Gasification	Entrained Flow gasification. 29.11 wt% water/70.88 wt% waste tire, P = 56 bar	[31]
	Oxygen to Tire ratio: 0.91, Ash melting energy: (1.0 kJ/kg_{ash})	[32]
COS hydrolysis	T = 200 °C, P = 54 bar	
H_2S removal	Solvent composition: 62.3 mol% DEPG: 37.7 mol% H_2O	[33]
	T = 40 °C, 53.5 bar, Removal: 92.7 % of H_2S	
Claus process	Two-stage sulfur conversion, Furnace: T = 950 °C	[34]
Natural Gas Converter		
NG pre-heater & pre-reformer	Pre-heater outlet T = 550 °C, Pre-reformer: T = 550 °C, P = 29.8 bar, Steam to NG ratio: 0.2	[1]
NG reformer	Autothermal reformer, Steam to NG ratio: 0.75, Oxygen to NG ratio: 0.95, Raw syngas cooled, dried & compressed to 55 bar	[1]
Air Separation Unit (ASU)	Oxygen purity: 99.5 mol%, Recovery pressure P = 10 bar	[6, 35]
Water Gas Shift (WGS)	High temperature WGS: T = 420 °C, P = 54 bar	[1, 6]
CO_2 removal	Solvent composition: 63.9 mol% DEPG: 36.1 mol% H_2O	[33]
	T = 20 °C, P = 53.5 bar, Removal: 96.9 % of CO_2	
Methanation	Four-stage conversion, Inlet T = 300 °C, Inlet P = 53.6 bar.	[36]
	Adiabatic reactors. Total ΔP = 3 bar (across 4 stages), Recycle ratio = 75 %	
SNG compression & purification	Outlet pressure = 55 bar	[34, 3]
SNG liquefaction	SNG flow rate = 9.7 kg/s, P = 55 bar, Inlet T = 22 °C, Outlet T = -157 °C	[29]
	MSHE UA_{max} = 25.0 MW/K, Pressure ratio = 6.5	
	Refrigerant mole composition: N_2: 8.3, CH_4: 24.0, C_2H_6: 36.9, n-C_4H_{10}: 30.8	
	Low P = 2.8 bar, high P = 18.0 bar, ΔT_{min} = 0.95 K, Flow rate = 58.5 kg/s	
Methanol synthesis & purification	T = 240 °C, P = 51 bar, Recycle ratio = 85 %, Off-gases to GT, Purity: 99.5 mol%	[37, 38]
DME synthesis & purification	T = 280 °C, P = 50 bar, Off-gases to GT	[38, 39]
	DME Purification column, Purity: 99.5 mol%	
MTO & purification	T = 400 °C, P = 40 bar, Off-gases to GT	[40]
	CO_2 absorption unit. Absorbent: 70.0 wt% DGA: 30.0 wt% H_2O, Absorber: 2 bar, Regenerator: 1.5 bar, Purity 99.9 mol%	
	De-ethanizer, 35 bar Ethane recovery: 99.80 %, Power consumption: 0.35 $MWe/MW_{LHV,Ethane}$	
	De-methanizer, 34 bar Methane removal: 99.99 % Power consumption: 1.21 $MWe/MW_{LHV,Methane}$	
	C2-splitter, 10 bar, Ethylene recovery: 95.00 %, purity: 99.9 mol%, Power consumption: 0.64 $MWe/MW_{LHV,Ethylene}$	
	De-propanizer, 25 bar, Propylene recovery: 98.00 %, purity: 99.2 mol%	
Gas Turbine	Thermal Efficiency: 46.8 % (Ratio of Net Power out [MW] to Total LHV of input fuel)	Simulation
Steam Turbine	Thermal Efficiency (High Quality heat): 44.1 %, Thermal Efficiency (Low Quality heat): 15.4 % (Details in Supp. Mat.)	[41, 42]
Postcombustion CO_2 capture	Solvent composition: 72.3 wt% DGA: 27.3 wt% H_2O	[33, 3]
	T = 70 °C, P = 1.0 bar, CO_2 Removal = 95.0 %	
CO_2 compression	Multistage compressors, CO_2 purity = 99.1 mol%, Outlet T = 25 °C, P = 153 bar	[35]
CO_2 transportation and sequestration	Operating cost: 12.5 $/tonne	[1]
Compressors	Isentropic efficiency = 80 %, maximum pressure ratio = 5	[1]
Pumps	Efficiency = 80 %	[1]

Table 1: Operating parameters and specifications used for the rigorous process simulation

3. Optimization Problem Formulation

3.1. Process Simulation and Surrogate Model

3.1.1. General description

Figure 1 presents a superstructure of the hybrid natural gas and solid waste tire feedstock polygeneration process that produces the following product portfolio: Electricity, liquefied (synthetic or well) natural gas, methanol, dimethyl ether, ethylene and propylene. Rigorous mass and energy balance models for the various sections of the superstructure are developed using either Aspen HYSYS v10 (for Selexol units) or Aspen Plus v10 (for all other units); an overview of the operating conditions used is presented in Table 1. A detailed presentation of the process modeling and simulation strategy is available in our previous work ([4] and [43]) where global optimization was performed without consideration of uncertainty. However, certain simplifications are made in the current work in order to keep the optimization problem computationally tractable when uncertainty is considered. An overview of the process model and changes made is presented next.

Operational decision variables for each scenario ($\mathbf{x}_h$) are presented in red in Figure 1 and described in Table 2. The total thermal input of the entire plant in each scenario h is determined by two (extensive) decision variables: The mass flow rates of waste tire ($m_{tire,h}$) and natural gas ($m_{NG,h}$). This plantwide thermal input is constrained to be less than 893 MW so as to provide a fair comparison with both our previous work ([3, 4, 43]) as well as a benchmark paper by Larson et al. [44]. All other operational decision variables are intensive.

3.1.2. Waste Tire train

In Figure 1, we define a nonstandard block termed "Aggregate Waste Tire Converter" that encompasses four sub-blocks. The first is a tire feedstock and slurry preparation unit in which rubber is separated out, ground into crumbs and mixed with water. The crumb tire slurry and oxygen from an air separation unit (ASU) are fed into the second sub-block consisting of an entrained flow gasifier (housed together with the radiant syngas cooling and quench system) that generates raw syngas. The third sub-block performs syngas cleaning and consists of a scrubber (for removal of particulates, sulfides and chlorides), COS hydrolysis (to H_2S) unit, syngas cooler and sour water knockout drum, a Selexol-based H_2S removal unit and a Claus unit (for conversion of captured H_2S to elemental sulfur). Slag flows down the

walls of the gasifier and falls down into the quench where it solidifies. The solids and ash are removed and treated in the fourth sub-block.

Compared to our previous work, two simplifications are made: The ratio of the oxygen to tire mass flow rate is fixed and the option for sulfur removal is implemented immediately after the gasifier. Since all other relevant operating conditions are fixed, these two simplifications imply that the surrogate mass balance model takes the form of a linear function (Equation 1) relating the clean syngas mole flow rate in scenario h ($f_{TDsweet\_gas,i,h}$) to $m_{tire,h}$. All the constants such as the mole fraction of component i belonging to the component set I ($x_{TDsweet\_gas,i}$), molecular weight ($MW_{TDsweet\_gas}$) and syngas yield (R_{ST} - the ratio of the mass flow rates of clean syngas to tire) of the clean syngas stream are determined directly from the Aspen Plus simulation. The H_2/CO mole ratio of the clean tire-derived syngas stream is ~ 0.7. We note that making the first simplification eliminates the need to implement a highly nonlinear (and thus nonconvex) surrogate model to represent the complex gasification process as was done in [43]; we found that performing optimization under uncertainty with such a model was computationally intractable even for a small number of scenarios because convexifying these constraints yields only weak lower bounds which in turn implies that the set of feasible candidate solutions of the first-stage binary variables does not shrink sufficiently quickly. An analogous argument holds for developing the surrogate energy balance model. Similarly, implementing the sulfur removal system immediately after the gasifier eliminates the (nonconvex) bilinear terms associated with an additional stream splitter. In addition, for the case of flexible polygeneration, we expect it to be cheaper to implement a single high-throughput sulfur removal system prior to the stream splitter that operates in a large number of scenarios than to implement multiple sulfur removal systems in the methanation and methanol synthesis trains (as done in [43]) that each operate in a smaller number of scenarios even though the latter option eliminates the need for a dedicated COS hydrolysis reactor.

$$f_{TDsweet\_gas,i,h} = \frac{x_{TDsweet\_gas,i} \cdot R_{ST} \cdot m_{tire,h}}{MW_{TDsweet\_gas}},\ \forall i \in I, \forall h \in \{1, ..., s\} \qquad (1)$$

The clean tire-derived syngas stream is then split into three branches heading to the methanation, gas turbine and methanol synthesis sections with the corresponding stream split fractions in scenario h denoted by $S_{TSNG,h}$, $S_{TGT,h}$ and $S_{TMeOH,h}$ respectively. The mass balance constraints are presented in Equation 2, where $f_{TMETH\_feed,i,h}$, $f_{TGT\_feed,i,h}$ and $f_{TMEOH\_feed,i,h}$ denote the

molar flow rates of component i in the tire-derived syngas stream heading to the methanation, gas turbine and methanol synthesis sections in scenario h respectively. We note that the bilinear terms in Equation 2 introduce nonconvexities; the reformulation-linearization technique (RLT) is used to generate a set of auxiliary mass balance constraints for the splitter that yield tighter convex relaxations for the lower bounding problem as presented in Section 3.1.6.

$$\begin{gathered} f_{TMETH\_feed,i,h} = f_{TDsweet\_gas,i,h} \cdot S_{TSNG,h},\ \forall i \in I, \forall h \in \{1, ..., s\} \\ f_{TGT\_feed,i,h} = f_{TDsweet\_gas,i,h} \cdot S_{TGT,h},\ \forall i \in I, \forall h \in \{1, ..., s\} \\ f_{TMEOH\_feed,i,h} = f_{TDsweet\_gas,i,h} \cdot S_{TMeOH,h},\ \forall i \in I, \forall h \in \{1, ..., s\} \\ S_{TSNG,h} + S_{TGT,h} + S_{TMeOH,h} = 1.0, \forall h \in \{1, ..., s\} \end{gathered} \tag{2}$$

3.1.3. Natural gas train

An analogous modeling approach is followed for the natural gas train: The natural gas feedstock is split into three streams that head to the liquefaction, gas turbine and methanol synthesis sections with the corresponding split fractions given by $S_{NGLiq,h}$, $S_{NGGT,h}$ and $S_{NGRef,h}$ respectively. Mass balance constraints of a similar form to Equation 2 together with auxiliary RLT constraints are implemented. For the natural gas stream heading to the methanol synthesis section, a block termed "Aggregate Natural Gas Converter" is defined that encompasses the natural gas pre-heater and pre-reformer, the reformer, scrubber and compressor for natural gas-derived syngas. Similar to the waste tire train, in this work we implement simpler linear surrogate mass and energy balance models for the natural gas conversion section by fixing the ratios of the converted natural gas stream and the steam and oxygen flow rates fed to the reformer. This yields a natural gas-derived syngas stream with a H_2/CO mole ratio of ~ 3.0.

3.1.4. Product synthesis trains

Tire-derived syngas heading to the methanation or methanol synthesis sections can be upgraded using a water gas shift (WGS) reactor; the overall conversion of CO in scenario h is an operational decision variable denoted by $c_{SNGWGS,h}$ and $c_{MeOHWGS,h}$ respectively. Prior to methanation, CO_2 is removed in a Selexol-based process. The H_2/CO mole ratio of the stream

heading to the first methanation reactor is constrained to be ~ 3.0. The produced synthetic natural gas stream is combined with the relevant natural gas branch prior to liquefaction to produce liquified natural gas (LNG). Conversely, in the methanol synthesis train, the natural gas-derived syngas stream is blended with the (upgraded) tire-derived syngas stream first before heading to the CO_2 removal and methanol synthesis sections. The H_2/CO mole ratio of the stream heading to the methanol synthesis reactor is constrained to be ~ 2.0. Thus this correct ratio can be attained either by using the appropriate tire and natural gas flow rates (and thereby exploiting synergies between the two feedstocks) or by employing the WGS reactor. For each scenario h, the produced methanol stream either heads to the DME synthesis section, the MTO section or is directly sold as the final product with the corresponding split fractions denoted by $S_{DME,h}$, $S_{MTO,h}$ and $S_{MeOHProd,h}$ respectively. This methanol splitter is modeled using a mass balance model similar to Equation 2 together with auxiliary RLT constraints. We note that with the exception of the stream splitter model, all other mass and energy balance constraints in the methanation and methanol synthesis trains are linear.

3.1.5. Power generation and CO_2 capture trains

For the gas turbine section, energy balance constraints are implemented by assuming a constant gas turbine efficiency such that the net work generated in each scenario is a linear function of the total thermal input (on a LHV basis) of the relevant natural gas and tire-derived syngas streams. A similar approach is used to determine the additional electricity generated in the steam turbine utilizing waste heat from the flue gas. The flue gas stream is either emitted or heads to a DGA-based postcombustion CO_2 capture unit with corresponding split fractions given by $S_{PostEm,h}$ or $S_{PostCCS,h}$ respectively. Similarly, the captured CO_2 streams from the Selexol units are either emitted or head to the CO_2 compression and liquefaction system with corresponding split fractions given by $S_{PreEm,h}$ and $S_{PreCCS,h}$ respectively. Both these splitters result in nonconvex mass balance constraints similar to Equation 2 in addition to RLT constraints.

3.1.6. Auxiliary Reformulation-Linearization Technique (RLT) constraints

The nonconvex bilinear terms introduced in Equation 2 potentially yield weak convex relaxations when constructing the lower bounding problem. This may result in slow convergence of the NGBD algorithm. Thus, it is

essential to augment the optimization model with relevant reformulation-linearization technique (RLT) constraints as detailed in [25] and [45]. These are a set of constraints that are redundant for the original Problem (SP) but are not redundant for its convex relaxation thereby yielding a tighter lower bounding problem. For the specific case of bilinear terms, the RLT constraints derived by Quesada and Grossmann are implemented which take the form of Equation 3 (corresponding to the constraints of Equation 2) [46]. Similar RLT constraints are implemented for the other equations involving bilinear terms. We note that Equation 3 has a physical interpretation as an alternative formulation of the splitter mass balance constraints although this is not always the case for other kinds of nonconvexities.

$$f_{TDsweet\_gas,i,h} = f_{TMETH\_feed,i,h} + f_{TGT\_feed,i,h} + f_{TMEOH\_feed,i,h}, \quad \forall i \in I, \forall h \in \{1, ..., s\} \tag{3}$$

3.2. Economic Model

3.2.1. Uncertainty Characterization

Table 3 presents the vector of uncertain parameters considered in this work which consists of the following components: The market prices of the six products, the waste tire tipping fees and the prevailing CO_2 tax rate. The uncertain parameter vector is assumed to be a random vector belonging to a normal distribution with the means and standard deviations listed in Table 3. The values for the means and standard deviations are determined from historical data obtained from the sources listed. The uncertain parameter vector ($\boldsymbol{\omega}_h$) is assumed to take on one of a finite number of scenarios s sampled from the normal distribution according to the approach presented by Li et al. [12]. Two different values of s are studied: 256 (2 scenarios for each of the 8 uncertain parameters) and 864 (3 scenarios for $P_{Elec,h}$, $P_{MeOH,h}$, $P_{Tire,h}$ and only 2 scenarios for the other uncertain parameters so as solve the problem in reasonable computation times). Furthermore, two cases are studied in this work. Case 1 investigates the optimization under uncertainty problem using the historical mean and standard deviation values presented in Table 3. However, in the interest of investigating the influence of higher volatility in market conditions, we also study an additional case (Case 2) in which the uncertain parameters have the same mean values as Case 1 but have higher standard deviations by 25%.

3.2.2. Expected Net Present Value (NPV) calculation

The objective of the optimization problem is to maximize the expected NPV of the flexible polygeneration plant as presented in Problem (FP). NPV is calculated using the Discounted Cash Flow Rate of Return approach with the assumptions made in [18] where R_{tax}, r, t_{dp} and t_{lf} denote the income tax rate, annual discount rate, depreciation time and project lifetime respectively.

Cap denotes the total capital cost. The polygeneration plant consists of 20 process sections (collected into a set U) and each section u can take on one size out of a discrete set of section sizes as presented in Equation 4, where $S_{u,j}$ is the j^{th} choice for size of the section, S_u^{LBD} and S_u^{UBD} are the lower and upper bounds on the section size, and d is the number of equipment sizes available (i.e., the cardinality of the discrete set of sizes) which is fixed to be 10 to keep the problem tractable.

$$S_{u,j} = S_u^{LBD} + \frac{j-1}{d-1} \cdot (S_u^{UBD} - S_u^{LBD}),\ \forall u \in U,\ \forall j \in \{1, ..., d\} \tag{4}$$

The capital cost associated with each section size $S_{u,j}$ (denoted $Cap_{u,j}$) is given by Equation 5, where $Cap_{u,0}$, $S_{u,0}$ and sf_u denote the base cost, base capacity and scaling factor of section u.

$$Cap_{u,j} = Cap_{u,0} \cdot \left(\frac{S_{u,j}}{S_{u,0}}\right)^{sf_u},\ \forall u \in U,\ \forall j \in \{1, ..., d\} \tag{5}$$

For each section u, the binary first-stage decision variables $y_{u,j}$ represents the choice of the j^{th} size, with $\mathbf{y}$ denoting a vector of these variables. Thus, the designed section size (S_u) and the corresponding capital cost (Cap_u) are presented in Equations 6 and 7 respectively, with Equation 8 representing the constraint that only one size can be chosen and Equation 9 giving the total capital costs (where K_L and K_{WC} are factors representing the additional costs associated with purchasing land and working capital).

$$S_u = \sum_{j=1}^{d} S_{u,j} \cdot y_{u,j},\ \forall u \in U \tag{6}$$

$$Cap_u = \sum_{j=1}^{d} Cap_{u,j} \cdot y_{u,j},\ \forall u \in U \tag{7}$$

$$\sum_{j=1}^{d} y_{u,j} = 1, \ \forall u \in U \tag{8}$$

$$Cap = (K_L + K_{WC}) \cdot \sum_{u \in U} Cap_u \tag{9}$$

The linking (complicating) constraints are presented in Equation 10, where the throughput for each section in scenario h ($F_{u,h}$) is constrained to be lower than the section's capacity.

$$F_{u,h} \leq S_u, \ \forall u \in U, \ \forall h \in \{1, ..., s\} \tag{10}$$

$Pro_{net,h}$ denotes the annual net profit in scenario h which is the difference between the annual revenues (from product sales and tipping fees) and the annual operating costs (consisting of variable operating costs such as feedstock costs, CO_2 taxes, utility, solvent, catalyst and waste disposal costs, and fixed operating costs including labor costs, operating overhead, property taxes and insurance). Details on the data and sources used for the economic model are presented in the Supplementary Material.

3.3. Summary of Optimization under Uncertainty Problem

Problem (FP) summarizes the flexible polygeneration problem which takes the form of a two-stage stochastic nonconvex MINLP. Problem (FP) has 200 binary first-stage decision variables, $435s$ continuous second-stage variables, 20 first-stage equality constraints, $412s$ second-stage equality constraints and $32s$ second-stage inequality constraints. We note that Problem (FP) has more than 100,000 variables and constraints (for $s = 256$) and close to 400,000 variables and constraints (for $s = 864$). The complete formulation of the optimization problem is presented in the Supplementary Material.

Operational decision variable ($\mathbf{x}_h$)	Description (for each scenario h $\in \{1, ..., s\}$)	Units	LBD	UBD
Waste tire train				
$m_{tire,h}$	Mass flow rate of waste tire	kg/s	0.0	26.3
$S_{TSNG,h}$	Split fraction of tire-derived syngas sent to methanation		0.0	1.0
$S_{TMeOH,h}$	Split fraction of tire-derived syngas sent to methanol synthesis		0.0	1.0
$S_{TGT,h}$	Split fraction of tire-derived syngas sent to the gas turbine		0.0	1.0
Natural gas train				
$m_{NG,h}$	Mass flow rate of natural gas	kg/s	0.0	18.7
$S_{NGRef,h}$	Split fraction of natural gas sent to reformer		0.0	1.0
$S_{NGGT,h}$	Split fraction of natural gas sent to gas turbine		0.0	1.0
$S_{NGLiq,h}$	Split fraction of natural gas sent for liquefaction		0.0	1.0
Downstream product trains				
$c_{SNGWGS,h}$	Overall conversion of CO in the WGS reactor prior to methanation		0.0	0.8
$c_{MeOHWGS,h}$	Overall conversion of CO in the WGS reactor prior to methanol synthesis		0.0	0.8
$S_{MeOHProd,h}$	Split fraction of methanol sold as product		0.0	1.0
$S_{DME,h}$	Split fraction of methanol sent to DME synthesis		0.0	1.0
$S_{MTO,h}$	Split fraction of methanol sent to MTO synthesis		0.0	1.0
CO_2 capture train				
$S_{PostCCS,h}$	Split fraction of flue gas sent to the DGA-based postcombustion CCS		0.0	1.0
$S_{PreCCS,h}$	Split fraction of CO_2 removed in other plant sections sent to sequestration		0.0	1.0
$S_{PostEm,h}$	Split fraction of flue gas sent to stack/emitted		0.0	1.0
$S_{PreEm,h}$	Split fraction of CO_2 removed in other plant sections sent to stack/emitted		0.0	1.0

Table 2: List of the 17 operating decision variables for the optimization problem

Uncertain parameter vector ($\boldsymbol{\omega}_h$)	Description	Units	Mean	Standard deviation	Source
$P_{NG,h}$ [1]	Natural gas price	\$/MMBtu	5.5	3.0	[47]
$P_{Elec,h}$	Hourly electricity price	\$/MWh	96.1	22.1	[48]
$P_{MeOH,h}$	Methanol price	\$/tonne	500	200	[49]
$P_{DME,h}$	DME price	\$/tonne	800	200	[50]
$P_{Ethylene,h}$	Ethylene price	\$/tonne	1050	360	[51]
$P_{Propylene,h}$	Propylene price	\$/tonne	1000	400	[52]
$P_{Tire,h}$	Waste tire tipping fee	\$/tonne	50	25	Assumed
$P_{CO_2,h}$	CO_2 tax rate	\$/tonne	50	25	Assumed

Table 3: Prices and CO_2 tax rate parameters for the scenarios. [1]A fixed premium of 65% is assumed for the price of LNG over the price of natural gas based on data from [47]

$$
\begin{aligned}
\max_{\mathbf{y},\mathbf{x}_1,\ldots,\mathbf{x}_s} \quad & \mathbb{E}_{\boldsymbol{\omega}}[\text{NPV}] = Cap(\mathbf{y}) \cdot \Big[-1 + \frac{R_{tax}}{r \cdot t_{dp}} \cdot \Big(1 - \frac{1}{(1+r)^{t_{dp}}}\Big)\Big] \\
& + \sum_{h=1}^{s} p_h \cdot Pro_{net,h}(\mathbf{x}_h, \boldsymbol{\omega}_h) \cdot \Big[\frac{1}{r} \cdot \Big(1 - \frac{1}{(1+r)^{t_{lf}}}\Big)\Big] \\
\text{s.t.} \quad & \text{First-stage constraints: Capital cost model,} \\
& \text{Second-stage constraints: Mass and energy balance model, } \forall h \in \{1,...,s\}, \\
& \qquad \text{Annual net profit model, Scale constraints, } \forall h \in \{1,...,s\}, \\
& \text{Linking constraints: Throughput}_h \leq \text{Equipment Capacity, } \forall h \in \{1,...,s\},
\end{aligned}
\tag{FP}
$$

4. Results and Discussion

4.1. Case 1: Using historical means and standard deviations

Table 4 presents the capital costs and expected operational characteristics of two proposed flexible polygeneration processes corresponding to the two characterizations of uncertainty studied (i.e., with 256 and 864 scenarios). For comparison, the results of the nominal design in which all uncertain parameters are assumed to take on their mean values are also presented. In the nominal (inflexible) design, methanol is favored as a primary product together with a small amount of electricity produced from combustion of off-gases and waste heat recovery. Both waste tire and natural gas are utilized as a feedstock with the syngas upgraded using a water gas shift reactor. We note that this outcome of production of only a single primary product by an inflexible design is consistent with previous empirical results [2, 4, 43, 18] as well as Proposition 1 of Farhat and Reichelstein [17].

In Flexible design 1, four products are produced in changing quantities over the plant life time: Liquified (S)NG, electricity, methanol and dimethyl ether. Thus, the operating conditions of the plant are adjusted in response to market conditions in order to produce the most profitable product portfolio at a given time. Higher capital investments are made at the design stage in order to provide this operational flexibility. In order to provide a fair comparison between the flexible and nominal design, the value of the stochastic solution (VSS as detailed in [20]) is calculated using Equation 11, where $\mathbb{E}_{\boldsymbol{\omega}}[\text{NPV}_{Flexible}]$ denotes the expected NPV of the flexible design and $\mathbb{E}_{\boldsymbol{\omega}}[\text{NPV}_{EVP}]$ denotes the expected NPV of the expected value problem (also

termed the expectation of the expected value problem). The expected value problem is formulated by fixing the first-stage design variables to those obtained with the nominal design; the stochastic program is then run with the same uncertainty characterization as the flexible design. Thus, the expectation of the expected value problem gives the NPV that would be obtained if the nominal design faces uncertainty belonging to the same distribution as that faced by the flexible design. Table 4 shows that implementing flexible designs gives a substantial VSS highlighting the importance of taking uncertainty into account.

$$\text{VSS} = \mathbb{E}_{\boldsymbol{\omega}}[\text{NPV}_{Flexible}] - \mathbb{E}_{\boldsymbol{\omega}}[\text{NPV}_{EVP}] \tag{11}$$

The expected product portfolio and operational characteristics are also presented which corresponds to the weighted average (by probability) over all scenarios of the values of the given operational variable. For each product, the terms in parenthesis denote the percentage of scenarios (weighted by probability) in which the product is produced. For instance, for Flexible design 1, this implies that electricity is produced in all scenarios, liquified (S)NG is produced in only 12.5 % of scenarios while methanol and DME are produced in half of all scenarios. We note that this implies that there exist certain scenarios in which liquified (S)NG is produced together with one of methanol or DME. Such a product portfolio may be attained in a scenario that primarily favors methanol (or DME) which is produced using most of the feedstock (by thermal input). However, given the discrete set of equipment sizes, a small amount of natural gas (corresponding to the difference between the maximum allowable thermal input and the thermal input used to produce methanol or DME) may head to the relatively cheap liquefaction section.

4.2. Case 2: Assuming 25 % higher standard deviations

Table 5 presents the corresponding results for the case with higher assumed variances (i.e., higher volatility) for all uncertain parameters. We note that the mean values of the uncertain parameters are unchanged thus the nominal design is identical to Case 1.

For Flexible design 1, the same design as in Case 1 is proposed but the plant attains a higher expected NPV. This can be explained as follows: For a scenario in which one product experiences an unusually high price, that product is favored. However, if that product experiences an unusually low price, operating conditions are adjusted to favor a different product in the

portfolio. For Flexible design 2, the solution favors implementing a larger aggregate waste tire converter to provide additional operational flexibility. This results in a higher expected production of electricity relative to Case 1. In Case 2, Flexible designs 1 and 2 result in a higher expected NPV compared to the corresponding flexible designs in Case 1. We note that this result of attaining a higher expected NPV with increasing price volatility (around the same mean) is consistent with Proposition 2a of Farhat and Reichelstein [17]. The VSS also increases compared to Case 1.

Case 1		Nominal design	Flexible design 1	Flexible design 2
Number of scenarios s		1	256	864
Capital costs				
Aggregate Waste Tire Converter	M$	198.2	198.2	198.2
Aggregate Natural Gas Converter	M$	60.0	60.0	60.0
Liquified (Synthetic) Natural Gas train				
Water Gas Shift 1	M$	0.0	0.0	0.0
CO_2 removal	M$	0.0	0.0	0.0
Methanation	M$	0.0	0.0	0.0
Liquefaction	M$	0.0	24.9	0.0
Methanol train				
Water Gas Shift 2	M$	9.7	9.7	9.7
CO_2 removal	M$	13.7	13.7	13.7
Methanol synthesis	M$	81.2	81.2	81.2
Dimethyl Ether (DME) synthesis	M$	0.0	100.5	100.5
Methanol-To-Olefins (MTO) process	M$	0.0	0.0	0.0
Power system [1]	M$	110.2	110.2	110.2
Post-combustion CO_2 capture	M$	0.0	0.0	0.0
CO_2 compression & sequestration	M$	4.6	4.6	4.6
Air Separation Unit	M$	164.6	164.6	164.6
Water systems	M$	63.2	77.4	77.4
Miscellaneous [2]	M$	52.6	52.6	52.6
Total capital costs (Cap)	M$	758.0	897.5	872.6
Expected product portfolio[3]				
Liquefied (S)NG	kg/s	0.0	1.4 (12.5 %)	0.0
Electricity	MW	14.2 (100 %) [4]	20.4 (100.0 %)	17.8 (100.0 %)
Methanol	kg/s	28.2 (100 %)	14.2 (50.0 %)	14.2 (50.0 %
Dimethyl Ether	kg/s	0.0	7.0 (50.0 %)	8.2 (50.0 %)
Ethylene	kg/s	0.0	0.0	0.0
Propylene	kg/s	0.0	0.0	0.0
Expected process operation				
Waste tire used	kg/s	10.0	9.2	9.1
Natural gas used	kg/s	11.6	12.1	11.8
Direct CO_2 emissions	kg/s	5.1	11.9	10.7
CO_2 sequestered	kg/s	13.8	6.2	7.3
Annual Net Profit	M$/year	155.4	231.8	214.4
Net Present Value (NPV)	M$	485.6	931.5	824.4
Expectation of expected value problem	M$	-	613.4	564.2
Value of the Stochastic Solution (VSS)	M$	-	318.1	260.2
Total wall time (NGBD)	s	155.2	3033.7	3219.6
Total wall time (ANTIGONE)	s	1.5	[5]	[5]

Table 4: Capital costs and expected operational characteristics of the two proposed flexible polygeneration processes compared with the nominal design for uncertainty characterized using historical means and standard deviations. [1] Includes the Gas Turbine, HRSG, Steam Turbine and Electricity accessory costs. [2] Miscellaneous includes Instrumentation & Control, Site preparation & improvement and Building & Structures. [3] The expected operational characteristic corresponds to the weighted average (by probability) over all scenarios of the values of the given operational variable. [4] The terms in parenthesis denote the percentage of scenarios (weighted by probability) in which the corresponding product is produced. [5] ANTIGONE was unable to provide a solution in 15,000 s.

Case 2		Nominal design [6]	Flexible design 1	Flexible design 2
Number of scenarios s		1	256	864
Capital costs				
Aggregate Waste Tire Converter	M$	198.2	198.2	322.0
Aggregate Natural Gas Converter	M$	60.0	60.0	60.0
Liquified (Synthetic) Natural Gas train				
Water Gas Shift 1	M$	0.0	0.0	0.0
CO_2 removal	M$	0.0	0.0	0.0
Methanation	M$	0.0	0.0	0.0
Liquefaction	M$	0.0	24.9	0.0
Methanol train				
Water Gas Shift 2	M$	9.7	9.7	9.7
CO_2 removal	M$	13.7	13.7	22.3
Methanol synthesis	M$	81.2	81.2	81.2
Dimethyl Ether (DME) synthesis	M$	0.0	100.5	100.5
Methanol-To-Olefins (MTO) process	M$	0.0	0.0	0.0
Power system [1]	M$	110.2	110.2	110.2
Post-combustion CO_2 capture	M$	0.0	0.0	0.0
CO_2 compression & sequestration	M$	4.6	4.6	5.8
Air Separation Unit	M$	164.6	164.6	164.6
Water systems	M$	63.2	77.4	77.4
Miscellaneous [2]	M$	52.6	52.6	52.6
Total capital costs (Cap)	M$	758.0	897.5	1006.2
Expected product portfolio[3]				
Liquefied (S)NG	kg/s	0.0	1.5 (12.5 %)	0.0
Electricity	MW	14.2 (100 %) [4]	20.8 (100 %)	22.6 (100 %)
Methanol	kg/s	28.2 (100 %)	14.2 (50.0 %)	13.3 (50.0 %
Dimethyl Ether	kg/s	0.0	6.9 (50.0 %)	7.9 (50.0 %)
Ethylene	kg/s	0.0	0.0	0.0
Propylene	kg/s	0.0	0.0	0.0
Expected process operation				
Waste tire used	kg/s	10.0	9.1	14.0
Natural gas used	kg/s	11.6	12.2	8.5
Direct CO_2 emissions	kg/s	5.1	11.9	15.0
CO_2 sequestered	kg/s	13.8	6.0	9.4
Annual Net Profit	M$/year	155.4	254.9	248.3
Net Present Value (NPV)	M$	485.6	1,104.6	958.2
Expectation of expected value problem	M$	-	699.7	627.3
Value of the Stochastic Solution (VSS)	M$	-	404.9	330.9
Total wall time (NGBD)	s	155.2	2277.2	2955.4
Total wall time (ANTIGONE)	s	1.5	[5]	[5]

Table 5: Capital costs and expected operational characteristics of the two proposed flexible polygeneration processes compared with the nominal design for uncertainty characterized using historical means but with standard deviations assumed to be 25 % higher than average. [1] Includes the Gas Turbine, HRSG, Steam Turbine and Electricity accessory costs. [2] Miscellaneous includes Instrumentation & Control, Site preparation & improvement and Building & Structures. [3] The expected operational characteristics correspond to the weighted average (by probability) over all scenarios of the values of the given operational variable. [4] The terms in parenthesis denote the percentage of scenarios (weighted by probability) in which the corresponding product is produced. [5] ANTIGONE was unable to provide a solution in 15,000 s. [6] The nominal design is identical to that of Case 1.

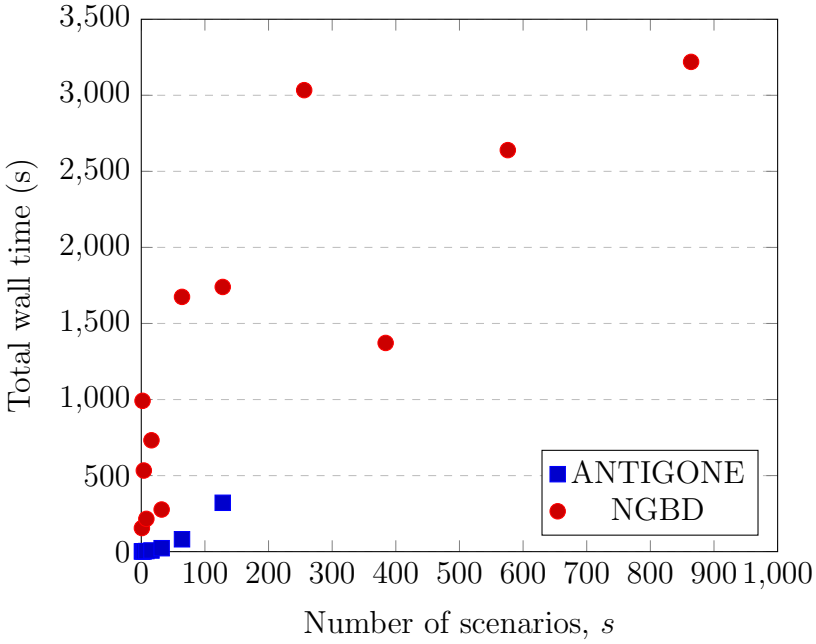

Figure 2: Scaling of solution times of NGBD and ANTIGONE with the number of scenarios

4.3. Computational Performance

Figure 2 presents the scaling of solution times of NGBD and ANTIGONE with number of scenarios. The procedure to generate these scenarios is presented in the Supplementary Material. When more than 128 scenarios are considered, ANTIGONE is unable to locate the global optimum within 15,000 s. Thus, NGBD scales favorably compared to ANTIGONE as the optimization under uncertainty problem becomes larger. However, NGBD performs worse than ANTIGONE for a smaller number of scenarios as the set of feasible candidate solutions of the first-stage binary variables does not shrink sufficiently quickly. We note that implementing RLT constraints was essential for convergence of NGBD in reasonable time.

5. Conclusions

The optimal design and operation under uncertainty of a hybrid feedstock flexible polygeneration system with a product portfolio consisting of electricity, methanol, dimethyl ether, olefins or liquefied (synthetic) natural gas is studied. The optimization problem is formulated as a recourse-based

two-stage stochastic nonconvex MINLP with first-stage variables corresponding to design decisions and second-stage variables to operational decisions. The recently developed GOSSIP software framework is used to model and efficiently solve the resulting formulations using the NGBD algorithm.

Two different characterizations of uncertainty are studied: In the first case study, the uncertain parameters are assumed to belong to independent normal distributions with means and standard deviations estimated using historical data. In the second case study, the standard deviations of the uncertain parameters are increased by 25 % in order to evaluate the impact of higher volatility. For each of these two cases, two flexible designs are developed based on a different number of scenarios. Implementing flexible designs is shown to result in an increase of expected net present value (compared to a nominal inflexible design) as well as a value of the stochastic solution in the range of 260 - 405 M$ for a scale of approximately 893 MW of thermal energy input. Price volatility around the same mean is shown to result in higher expected net present value and value of the stochastic solution as operational flexibility allows for asymmetric exploitation of price peaks.

Acknowledgements

A.S. gratefully acknowledges the financial support from NTNU's Department of Energy and Process Engineering and from NTNU Energy. R.K. gratefully acknowledges the support of the U.S. Department of Energy through the LANL/LDRD Program and the Center for Nonlinear Studies. This publication has been funded by HighEFF - Centre for an Energy-Efficient and Competitive Industry for the Future. The authors gratefully acknowledge the financial support from the Research Council of Norway and user partners of HighEFF, an 8-years Research Centre under the FME-scheme (Centre for Environment-friendly Energy Research, 257632).

Conflicts of Interest

The authors declare no conflicts of interest.

References

[1] T. A. Adams II, P. I. Barton, Combining coal gasification and natural gas reforming for efficient polygeneration, Fuel Processing Technology 92 (2011) 639–655.

[2] T. A. Adams II, J. H. Ghouse, Polygeneration of fuels and chemicals, Current Opinion in Chemical Engineering 10 (2015) 87–93.

[3] A. S. R. Subramanian, T. Gundersen, T. A. Adams II, Technoeconomic analysis of a waste tire to liquefied synthetic natural gas (SNG) energy system, Energy (2020) 117830.

[4] A. S. R. Subramanian, T. Gundersen, T. A. Adams II, Optimal design and operation of a waste tire feedstock polygeneration system, Energy (2021) 11990.

[5] A. M. Niziolek, O. Onel, M. F. Hasan, C. A. Floudas, Municipal solid waste to liquid transportation fuels–part ii: Process synthesis and global optimization strategies, Computers & Chemical Engineering 74 (2015) 184–203.

[6] I. J. Okeke, T. A. Adams II, Combining petroleum coke and natural gas for efficient liquid fuels production, Energy 163 (2018) 426–442.

[7] Y. K. Salkuyeh, T. A. Adams II, Integrated petroleum coke and natural gas polygeneration process with zero carbon emissions, Energy 91 (2015) 479–490.

[8] J. D. Martínez, N. Puy, R. Murillo, T. García, M. V. Navarro, A. M. Mastral, Waste tyre pyrolysis: A review, Renewable and Sustainable Energy Reviews 23 (2013) 179–213.

[9] V. Belgiorno, G. De Feo, C. Della Rocca, R. Napoli, Energy from gasification of solid wastes, Waste management 23 (2003) 1–15.

[10] J. F. Benders, Partitioning procedures for solving mixed-variables programming problems, Numerische mathematik 4 (1962) 238–252.

[11] A. M. Geoffrion, Generalized Benders decomposition, Journal of Optimization Theory and Applications 10 (1972) 237–260.

[12] X. Li, A. Tomasgard, P. I. Barton, Nonconvex Generalized Benders Decomposition for stochastic separable mixed-integer nonlinear programs, Journal of Optimization Theory and Applications 151 (2011) 425.

[13] X. Li, A. Sundaramoorthy, P. I. Barton, Nonconvex Generalized Benders Decomposition, in: Optimization in Science and Engineering, Springer, 2014, pp. 307–331.

[14] R. Kannan, Algorithms, analysis and software for the global optimization of two-stage stochastic programs, Ph.D. thesis, Massachusetts Institute of Technology, 2017.

[15] J. Meerman, A. Ramírez, W. Turkenburg, A. Faaij, Performance of simulated flexible integrated gasification polygeneration facilities. Part A: A technical-energetic assessment, Renewable and Sustainable Energy Reviews 15 (2011) 2563–2587.

[16] J. Meerman, A. Ramírez, W. Turkenburg, A. Faaij, Performance of simulated flexible integrated gasification polygeneration facilities, part b: Economic evaluation., Renewable and Sustainable Energy Reviews 16 (2012) 6083–6102.

[17] K. Farhat, S. Reichelstein, Economic value of flexible hydrogen-based polygeneration energy systems, Applied Energy 164 (2016) 857–870.

[18] Y. Chen, T. A. Adams II, P. I. Barton, Optimal design and operation of flexible energy polygeneration systems, Industrial & Engineering Chemistry Research 50 (2011) 4553–4566.

[19] Y. Chen, X. Li, T. A. Adams II, P. I. Barton, Decomposition strategy for the global optimization of flexible energy polygeneration systems, AIChE Journal 58 (2012) 3080–3095.

[20] J. R. Birge, F. Louveaux, Introduction to stochastic programming, Springer Science & Business Media, 2011.

[21] C. Li, I. E. Grossmann, A Review of Stochastic Programming Methods for Optimization of Process Systems under Uncertainty, Frontiers in Chemical Engineering 2 (2020) 34.

[22] A. Mitsos, B. Chachuat, P. I. Barton, McCormick-based relaxations of algorithms, SIAM Journal on Optimization 20 (2009) 573–601.

[23] A. M. Geoffrion, Elements of large-scale mathematical programming Part I: Concepts, Management Science 16 (1970) 652–675.

[24] A. M. Geoffrion, Elements of large scale mathematical programming part II: Synthesis of algorithms and bibliography, Management Science 16 (1970) 676–691.

[25] M. Tawarmalani, N. V. Sahinidis, Convexification and global optimization in continuous and mixed-integer nonlinear programming: theory, algorithms, software, and applications, volume 65, Springer Science & Business Media, 2013.

[26] K. A. Khan, H. A. Watson, P. I. Barton, Differentiable McCormick relaxations, Journal of Global Optimization 67 (2017) 687–729.

[27] E. Balas, R. Jeroslow, Canonical cuts on the unit hypercube, SIAM Journal on Applied Mathematics 23 (1972) 61–69.

[28] R. Misener, C. A. Floudas, ANTIGONE: Algorithms for Continuous/Integer Global Optimization of Nonlinear Equations, Journal of Global Optimization 59 (2014) 503–526.

[29] H. A. Watson, M. Vikse, T. Gundersen, P. I. Barton, Optimization of single mixed-refrigerant natural gas liquefaction processes described by nondifferentiable models, Energy 150 (2018) 860–876.

[30] N. Sunthonpagasit, M. R. Duffey, Scrap tires to crumb rubber: feasibility analysis for processing facilities, Resources, Conservation and recycling 40 (2004) 281–299.

[31] M. C. Woods, P. Capicotto, J. L. Haslbeck, N. J. Kuehn, M. Matuszewski, L. L. Pinkerton, M. D. Rutkowski, R. L. Schoff, V. Vaysman, Cost and performance baseline for fossil energy plants, National Energy Technology Laboratory (2007).

[32] C. Kunze, H. Spliethoff, Modelling, comparison and operation experiences of entrained flow gasifier, Energy Conversion and Management 52 (2011) 2135–2141.

[33] T. A. Adams II, Y. K. Salkuyeh, J. Nease, Processes and simulations for solvent-based CO2 capture and syngas cleanup, in: Reactor and process design in sustainable energy technology, Elsevier, 2014, pp. 163–231.

[34] R. Brasington, J. Haslbeck, N. Kuehn, E. Lewis, L. Pinkerton, M. Turner, E. Varghese, M. Woods, Cost and Performance Baseline for Fossil Energy Plants — Volume 2: Coal to Synthetic Natural Gas and Ammonia, Technical Report, DOE/NETL-2010/1402, 2011.

[35] J. Klara, M. Woods, P. Capicotto, J. Haslbeck, N. Kuehn, M. Matuszewski, L. Pinkerton, M. Rutkowski, R. Schoff, V. Vaysman, Cost and performance baseline for fossil energy plants volume 1: Bituminous coal and natural gas to electricity. National Energy Technology Laboratory, Research and Development Solutions, LLC (RDS) (2007).

[36] N. Kezibri, C. Bouallou, Conceptual design and modelling of an industrial scale power to gas-oxy-combustion power plant, International Journal of Hydrogen Energy 42 (2017) 19411–19419.

[37] Y. Su, L. Lü, W. Shen, et al., An efficient technique for improving methanol yield using dual CO 2 feeds and dry methane reforming, Frontiers of Chemical Science and Engineering (2019) 1–15.

[38] Y. K. Salkuyeh, T. A. Adams II, A new power, methanol, and DME polygeneration process using integrated chemical looping systems, Energy conversion and management 88 (2014) 411–425.

[39] J. A. Scott, T. A. Adams II, Biomass-gas-and-nuclear-to-liquids (BGNTL) processes part I: Model development and simulation, The Canadian Journal of Chemical Engineering 96 (2018) 1853–1871.

[40] Y. Salkuyeh, T. A. Adams II, Co-production of olefins, fuels, and electricity from conventional pipeline gas and shale gas with near-zero CO2 emissions. Part I: process development and technical performance, Energies 8 (2015) 3739–3761.

[41] Y. Chen, Optimal design and operation of energy polygeneration systems, Ph.D. thesis, Massachusetts Institute of Technology, 2013.

[42] Y. Chen, T. A. Adams II, P. I. Barton, Optimal design and operation of static energy polygeneration systems, Industrial & Engineering Chemistry Research 50 (2010) 5099–5113.

[43] A. S. R. Subramanian, T. Gundersen, P. I. Barton, T. A. Adams II, Optimal design and operation of a hybrid waste tire and natural gas feedstock polygeneration system, In preparation (2021).

[44] E. D. Larson, H. Jin, F. E. Celik, Large-scale gasification-based coproduction of fuels and electricity from switchgrass, Biofuels, Bioproducts and Biorefining 3 (2009) 174–194.

[45] R. Misener, C. A. Floudas, GloMIQO: Global mixed-integer quadratic optimizer, Journal of Global Optimization 57 (2013) 3–50.

[46] I. Quesada, I. E. Grossmann, Global optimization of bilinear process networks with multicomponent flows, Computers & Chemical Engineering 19 (1995) 1219–1242.

[47] U.S. Energy Information Administration. Natural Gas Prices., https://www.eia.gov/dnav/ng/ng_pri_sum_dcu_nus_m.htm, 2020. [Online; accessed 11-June-2020].

[48] Ontario Independent Electricity System Operator (IESO). Hourly Ontario Energy Price, http://www.ieso.ca/en/Power-Data/Price-Overview/Hourly-Ontario-Energy-Price, 2020. [Online; accessed 11-June-2020].

[49] Methanex Monthly Average Regional Posted Contract Price History, https://www.methanex.com/our-business/pricing, 2020. [Online; accessed 11-June-2020].

[50] Alibaba. Dimethyl Ether Prices., https://www.alibaba.com/product-detail/Competitive-dimethyl-ether-prices_60506781674.html?spm=a2700.galleryofferlist.0.0.29d77a22XwD6XM, 2020. [Online; accessed 11-June-2020].

[51] Independent Commodity Intelligence Services. Ethylene US prices., https://www.icis.com/explore/commodities/chemicals/ethylene/us/, 2020. [Online; accessed 11-June-2020].

[52] Independent Commodity Intelligence Services. Propylene US prices., https://www.icis.com/explore/commodities/chemicals/propylene/us/, 2020. [Online; accessed 11-June-2020].